(12) INTERNATIONAL APPLICATION PUBLISHED UNDER THE PATENT COOPERATION TREATY (PCT)

(19) World Intellectual Property Organization
International Bureau

(43) International Publication Date
1 July 2004 (01.07.2004)

PCT

(10) International Publication Number
WO 2004/055733 A2

(51) International Patent Classification[7]: G06T 7/00

(21) International Application Number:
PCT/GB2003/005445

(22) International Filing Date:
12 December 2003 (12.12.2003)

(25) Filing Language: English

(26) Publication Language: English

(30) Priority Data:
0229338.9 17 December 2002 (17.12.2002) GB

(71) Applicant *(for all designated States except US)*: **QINETIQ LIMITED** [GB/GB]; 85 Buckingham Gate, London SW1E 6PD (GB).

(72) Inventors; and

(75) Inventors/Applicants *(for US only)*: **WATSON, Sharon, Katrina** [GB/GB]; QinetiQ Limited, Cody Technology Park, Rm 1010 Building A9, Ively Road, Farnborough, Hampshire GU14 0LX (GB). **WATSON, Graham, Howard** [GB/GB]; QinetiQ Limited, Cody Technology Park, Rm 1008 Building A9, Ively Road, Farnborough, Hampshire GU14 0LX (GB).

(74) Agent: **OBEE, Robert, W.**; IP QinetiQ Formalities, Cody Technology Park, A4 Building, Room G016, Ively Road, Farnborough, Hampshire GU14 0LX (GB).

(81) Designated States *(national)*: AE, AG, AL, AM, AT, AU, AZ, BA, BB, BG, BR, BW, BY, BZ, CA, CH, CN, CO, CR, CU, CZ, DE, DK, DM, DZ, EC, EE, EG, ES, FI, GB, GD, GE, GH, GM, HR, HU, ID, IL, IN, IS, JP, KE, KG, KP, KR, KZ, LC, LK, LR, LS, LT, LU, LV, MA, MD, MG, MK, MN, MW, MX, MZ, NI, NO, NZ, OM, PG, PH, PL, PT, RO, RU, SC, SD, SE, SG, SK, SL, SY, TJ, TM, TN, TR, TT, TZ, UA, UG, US, UZ, VC, VN, YU, ZA, ZM, ZW.

(84) Designated States *(regional)*: ARIPO patent (BW, GH, GM, KE, LS, MW, MZ, SD, SL, SZ, TZ, UG, ZM, ZW),

[Continued on next page]

(54) Title: IMAGE ANALYSIS

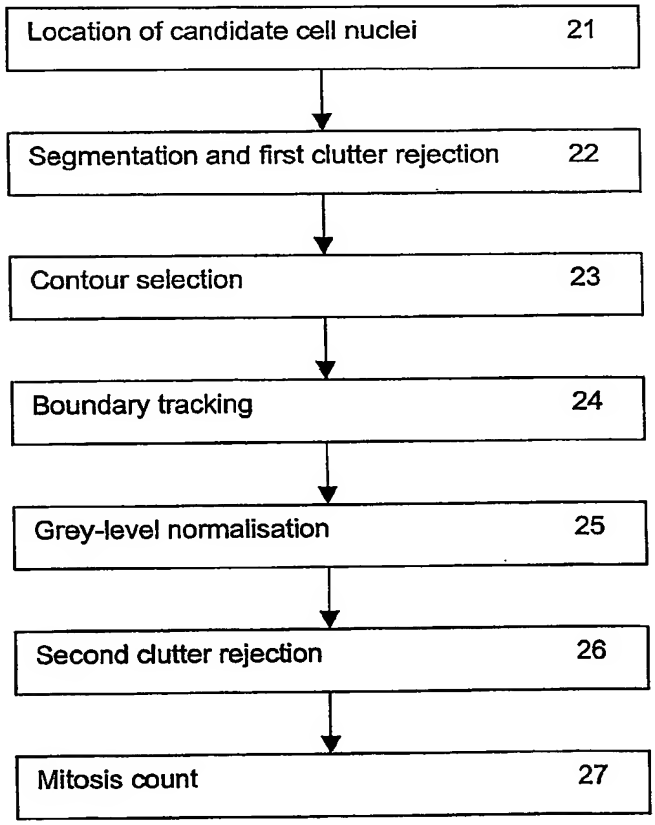

(57) Abstract: A method for the automated analysis of digital images, particularly for the purpose of assessing mitotic activity from images of histological slides for prognostication of breast cancer. The method includes the steps of identifying the locations of objects within the image which have intensity and size characteristics consistent with mitotic epithelial cell nuclei, taking the darkest 10 % of those objects, deriving contours indicating their boundary shape, and smoothing and measuring the curvature around the boundaries using a Probability Density Association Filter (PDAF). The PDAF output is used to compute a measure of any concavity of the boundary - a good indicator of mitosis. Objects are finally classified as representing mitotic nuclei or not, as a function of boundary concavity and mean intensity, by use of a Fisher classifier trained on known examples. Other uses for the method could include the analysis of images of soil samples containing certain types of seeds or other particles.

WO 2004/055733 A2

Eurasian patent (AM, AZ, BY, KG, KZ, MD, RU, TJ, TM), European patent (AT, BE, BG, CH, CY, CZ, DE, DK, EE, ES, FI, FR, GB, GR, HU, IE, IT, LU, MC, NL, PT, RO, SE, SI, SK, TR), OAPI patent (BF, BJ, CF, CG, CI, CM, GA, GN, GQ, GW, ML, MR, NE, SN, TD, TG).

Declaration under Rule 4.17:

— *of inventorship (Rule 4.17(iv)) for US only*

Published:

— *without international search report and to be republished upon receipt of that report*

For two-letter codes and other abbreviations, refer to the "Guidance Notes on Codes and Abbreviations" appearing at the beginning of each regular issue of the PCT Gazette.

Image Analysis

FIELD OF THE INVENTION

The present invention relates to the automated analysis of digital images. It is more particularly concerned with the automated identification of mitotic activity in digital images of histological or cytology specimens and most particularly for the purpose of assessing the presence and severity of cancer in breast tissue, and it is in this context that the invention is principally described herein. The invention may, however, also find application in the assessment of other forms of cancer, such as colon and cervical cancer, and in the analysis of various other kinds of structure presenting image components which are amenable to identification in a similar way, for example in the analysis of soil samples containing certain types of seeds or other particles.

BACKGROUND AND SUMMARY OF THE INVENTION

Many thousands of women die needlessly each year from breast cancer, a cancer from which there is theoretically a high probability of survival if detected sufficiently early. If the presence of cancerous tissue is missed in a sample, then, by the time the next test is undertaken, the cancer may have progressed and the chance of survival significantly reduced. The importance of detecting cancerous tissue in the samples can therefore not be over-emphasised.

A typical national breast screening programme uses mammography for the early detection of impalpable lesions. Once a lesion indicative of breast cancer is detected, then tissue samples are taken and examined by a trained histopathologist to establish a diagnosis and prognosis. More particularly, one of the principal prognostic factors for breast cancer is the extent of mitotic activity, that is to say the degree of epithelial cell division that is taking place. A histopathological slide is effectively a "snapshot" representing a very short time interval in a cell division process, so the chance of a particular slide showing a particular phase of mitotic activity is very small; if such a phase is in fact present in a slide, that is a good indicator of how fast a potential tumour is growing.

In the existing manual procedure for scoring mitotic activity a histopathologist places a slide under a microscope and examines a region of it (referred to as a tile) at a magnification of x40 for indications of mitoses. Typically ten different tiles from the tissue sample are examined and a total count is made of the number of cell divisions which, in the histopathologist's opinion, are seen to be taking place in the ten tiles. This is then converted to an indication of cancer grade typically in accordance with the following table:

Number of Mitotic Cells per Ten Tiles	**Cancer Grade**
0 to N	Grade 1
(N + 1) to M	Grade 2
> M	Grade 3

where Grade 1 is the least serious and Grade 3 is the most serious. Values of N and M are typically 5 and 10 but will vary in different schemes depending on the size of the tiles being observed.

This is, however, a time consuming, labour intensive and expensive process. Qualification to perform such examination is not easy to obtain and requires frequent review. The examination itself requires the interpretation of colour images by eye, a highly subjective process characterised by considerable variations in both inter, and intra-observer analysis, i.e. variances in observation may occur for the same sample by different histopathologists, and by the same histopathologist at different times. For example, studies have shown that two different histopathologists examining the same ten samples may give different opinions on three of them, an error of 30%. This problem is exacerbated by the complexity of some samples, especially in marginal cases where there may not be a definitive conclusion. If sufficient trained staff are not available this impacts upon pressures to complete the analysis, potentially leading to erroneous assessments and delays in diagnosis.

These problems mean that there are practical limitations on the extent and effectiveness of screening for breast cancer with the consequence that some women are not being correctly identified as having the disease and, on some occasions, this failure may result in premature death. Conversely, others are

being incorrectly diagnosed with breast cancer and are therefore undergoing potentially traumatic treatment unnecessarily.

It is thus an aim of the invention to provide an automated method of image analysis which can be embodied in a robust, objective and cost-effective tool to assist in the diagnosis and prognosis of breast cancer, although as previously indicated the invention may also find application in other fields.

In one aspect the invention accordingly resides in a method for the automated analysis of a digital image comprising an array of pixels, including the steps of: identifying the locations of objects within the image which have specified intensity and size characteristics; defining regions of specified extent within the image which contain respective said objects; deriving from the data within respective said regions one or more respective closed contours comprising points of equal intensities; and estimating the curvature of at least one respective said contour within respective said regions at least to produce a measure of any concavity thereof.

As will be understood from the ensuing detailed description of a preferred embodiment, such a method is of use in identifying mitotic cell nuclei in digital images of histopathological slides.

The invention also resides in apparatus for the automated analysis of a digital image comprising means to perform the foregoing method and in a computer program product comprising a computer readable medium having thereon computer program code means adapted to cause a computer to execute the foregoing method and in a computer program comprising instructions so to do.

These and other aspects of the invention will now be more particularly described, by way of example, with reference to the accompanying drawings and in the context of an automated system for grading cancer on the basis of the numbers of mitotic epithelial cell nuclei in digital images of histopathological slides of potential carcinomas of the breast.

BRIEF DESCRIPTION OF THE DRAWINGS

In the drawings:

Figure 1 is a block diagram of an automated process in accordance with the invention for measuring mitotic activity for patient diagnosis;

Figure 2 is a more detailed block diagram of the main stages in the mitosis detection and measurement block of Figure 1;

Figures 3 and 4 are simplified visualisations of the contour selection stage of the process of Figure 2; and

Figure 5 illustrates a decision boundary in a Fisher classifier as used in a later stage of the process of Figure 2.

DETAILED DESCRIPTION

Figure 1 shows a process for the assessment of tissue samples in the form of histopathological slides of potential carcinomas of the breast. The process measures mitotic activity of epithelial cells to produce a parameter for use by a pathologist as the basis for assessing patient diagnosis. It employs a database 1, which maintains digitised image data obtained from histological slides. Sections are cut from breast tissue samples (biopsies), placed on respective slides and stained using the staining agent Haematoxylin & Eosin (H&E), which is a common stain for delineating tissue and cellular structure.

To obtain the digitised image data for analysis, a histopathologist scans a slide under a microscope and at 40x magnification selects regions of the slide which appear to be most promising in terms of analysing mitotic activity. Each of these regions is then photographed using the microscope and a digital camera. In one example a Zeiss Axioskop microscope has been used with a Jenoptiks Progres 3012 digital camera. This produces for each region a respective digitised image in three colours, i.e. red, green and blue (R, G & B). Respective intensity values in the R, G and B image planes are thus obtained for each pixel in an array. In the preferred embodiment there is an eight-bit range of pixel intensities (values of 0 to 255) for each colour and the array comprises 1476 pixels across by 1160 pixels down, with a pixel size of 220nm square. The image data is stored temporarily at 1 for later use. Ten digitised images (electronic equivalents of tiles) are required for the detection and measurement of mitotic activity at 2, which then provides

input to a diagnostic report at 3. In principle the processing stages to be described in detail below can operate on a single waveband (R, G or B) image or a combination of them. In practice, however, the red waveband has been found to contain the most information for discriminating between mitotic and other cells when stained with H&E, and is assumed to be used in the following description. The process can be performed in a suitably programmed personal computer (PC) or other general purpose computer of suitable processing power or in dedicated hardware.

Figure 2 shows in more detail the processing stages comprised in the block 2 of Figure 1. They are carried out for each of the ten digitised images referred to above and will now be described for one such image (tile). To aid in the understanding of this description it is recalled that the aim of the process is to identify and count the number of mitotic epithelial cell nuclei (if any) in each tile. In images acquired as described above such nuclei generally appear darker than normal epithelial cell nuclei, and also have a different shape. Normal nuclei are generally convex with smooth boundaries while mitotic nuclei are more irregular in shape and have ragged boundaries. However, it is not always the case that mitotic epithelial cell nuclei are the darkest objects in a given tile; for example stromal cells, lymphocytes and necrotic cells may be darker. Given the relatively low numbers of mitoses which may be present in any given tile and yet may indicate serious disease it is important that as many as possible are correctly identified while at the same time minimising the number of any normal cell nuclei or other objects incorrectly identified as mitotic.

Location of candidate cell nuclei

Referring now to Figure 2, the first processing stage 21 consists of locating all possible candidate cell nuclei. The approach adopted for identifying the locations of potential mitotic nuclei is based on the fact that they are generally darker than average nuclei. Mitotic nuclei appear in the image as solid dark objects (i.e. dark all the way through) most of the time, or instead occasionally they form groups of small dark clumps. Hence the aim is to find concentrations of dark pixels; these are not necessarily connected groups of dark pixels, but a region containing a sufficient number of clustered dark pixels.

There are various methods of doing this. One example is simple grey-level segmentation, where a threshold is chosen and only those pixels having grey-

levels below this threshold are selected. The drawback of this approach is that some mitotic nuclei are not particularly dark, but are only distinguishable from their shape characteristics. Choosing a threshold sufficiently low to detect such nuclei would yield an excess of clutter.

The preferred approach is to use the multiresolution blob filtering described below. However, as will be apparent to those skilled in the image processing art, the present invention may be practised without employing this particular technique. Alternatives include the processes described as mitotic cueing in our copending United Kingdom patent application no. 0226787.0. The general principle is, given that the approximate size of the nuclei is known, to apply a radially-symmetric filter whose output is large in magnitude when there is a region of local brightness or darkness whose shape and size approximately matches that of the filter. This filter should be a difference filter with zero mean, so areas of constant intensity are suppressed.

The method will now be described in terms of a specific implementation, namely a multi-scale blob filter as known e.g. from "Multiresolution analysis of remotely sensed imagery", J.G.Jones, R.W.Thomas, P.G.Earwicker, Int J: Remote Sensing, 1991, Vol 12, No 1, pp 107-124. The process will be described for filtering the image using a particular size of blob filter, where these are defined at successive octave (powers of 2) scale sizes.

The recursive construction process for the multi-scale blob filter involves two filters; a 3x3 Laplacian blob filter (L) and a 3x3 smoothing filter (s) as defined below.

$$L=\begin{pmatrix}-1 & -1 & -1\\ -1 & 8 & -1\\ -1 & -1 & -1\end{pmatrix}, s=\frac{1}{16}\begin{pmatrix}1 & 2 & 1\\ 2 & 4 & 2\\ 1 & 2 & 1\end{pmatrix}$$

These two filters form a basis for filtering over a set of octave scale sizes, according to the following process:

To enhance blob-shaped objects at the original resolution (octave scale 1, pixel size 1), the image is correlated with the 3x3 Laplacian filter alone:

$$F_1(m,n)=\sum_{i=-1}^{1}\sum_{j=-1}^{1} I(m+i,n+j)*L(i+2,j+2)$$

where *I* is the original image, and the range of the indices *m* and *n* is set such that the indices in the summation above are always within the original image dimensions (so *m* and *n* start at 2). Values of the filtered image at locations outside these ranges are set to zero.

For computational efficiency, multiplications by ±1 need not be performed explicitly. Thus the filter output value for a pixel located at position (*i,j*) is given by:

$$F_1(i,j) = 8.I(i,j) - I(i-1,j-1) - I(i-1,j) - I(i-1,j+1) - I(i,j-1) - I(i,j+1) - I(i+1,j-1) - I(i+1,j) - I(i+1,j+1)$$

To enhance blob-shaped objects at a resolution one octave above the original (octave scale 2, pixel size 3), the image is first correlated with the 3x3 smoothing filter (*s*), forming a smoothed image (S_2). The 3x3 Laplacian blob filter (*L*) is then expanded by a factor of two, by padding it with zeros, to form a 5x5 filter [-1 0 -1 0 -1; 0 0 0 0 0; -1 0 8 0 -1; 0 0 0 0 0; -1 0 -1 0 -1]. This is then correlated with the smoothed image (S_2) to form a filtered image (F_2), but for computational efficiency, only the non-zero filter coefficients are used, thus:

$$S_2(m,n) = \sum_{i=-1}^{1}\sum_{j=-1}^{1} I(m+i,n+j) * s(i+2,j+2)$$

$$F_2(m,n) = \sum_{i=-1}^{1}\sum_{j=-1}^{1} S_2(m+2i,n+2j) * L(i+2,j+2)$$

where *I* is the original image, and the range of the indices *m* and *n* is set such that the indices in the summation above are always within the original image dimensions (so *m* and *n* start at 4). Values of the filtered image at locations outside these ranges are set to zero.

The above double correlation is equivalent to a single correlation of the original image with a 7x7 filter formed from correlating the expanded 5x5 Laplacian with the 3x3 smoothing filter, but this larger filter is never formed explicitly.

To enhance blob-shaped objects at a resolution two octaves above the original (scale 3, pixel size 7), the smoothing filter is expanded by a factor of 2 in the same manner as the Laplacian above, then correlated with the smoothed image (S_2) above to give a lower-resolution smoothed image (S_3) thus:

$$S_3(m,n) = \sum_{i=-1}^{1}\sum_{j=-1}^{1} S_2(m+2i,n+2j) * s(i+2,j+2)$$

Following this, the 5x5 Laplacian filter is expanded by a factor of 2 by padding with zeros to form a 9x9 filter, which is correlated with the smoothed image (S_3) in the same computationally efficient manner, thus:

$$F_3(m,n) = \sum_{i=-1}^{1}\sum_{j=-1}^{1} S_3(m+4i, n+4j) * L(i+2, j+2)$$

This process is repeated to obtain results at successive octave scales, namely expanding both the smoothing filter and the Laplacian blob filter each time.

The above process may be used to produce a "blob-filtered" image at any of the required octave scales. Objects of interest (i.e. clusters of dark pixels in this case) will have the greatest values of the magnitude of the filter output. The locally strongest filter output will occur at the centre of the object of interest. Individual objects (called "blobs") are now identified by finding local minima of the filter output, where each blob is assigned a position and intensity, the latter being the value of the filter output at the local minimum.

In this application, objects which are dark relative to the background are identified by finding local minima of the filter output at one chosen scale, in this instance octave scale 5 (a nuclear size of 31 pixels across).

For computational efficiency, the spatial resolution of the image is reduced prior to blob filtering, using the following thinning method. Each reduction in resolution by a factor of two (a "thin") is achieved by firstly correlating the image with the 3x3 smoothing filter (s), then sub-sampling by a factor of two. The formula for a single thin is:

$$T(m,n) = \sum_{i=-1}^{1}\sum_{j=-1}^{1} I(2m+i, 2n+j) * s(i+2, j+2)$$

where I is the original image, T is the thinned image, and the indices m and n range from 1 to the dimensions of the thinned image. Each dimension of the thinned image is given by subtracting 1 or 2 from the corresponding dimension of the original image, depending on whether this is odd or even respectively, then dividing by 2.

In this instance, the image is reduced in resolution by a factor of 4, by applying the above process twice, firstly on the original image, and then again on the resulting

thinned image, to produce a new image whose linear dimensions are a quarter of the size of the original (area is 1/16). For example, an original image of a tile of size 1476x1160 pixels would become 368x289 pixels. Blobs are now extracted as described above from the reduced-resolution image at octave scale 3 (7x7 pixels across), this being equivalent to extracting scale 5 blobs from the original image, but being more computationally efficient.

This process identifies all objects which form dark clusters of the requisite size, which may include not only mitotic epithelial cell nuclei but also background clutter, stromal cells, lymphocytes and/or necrotic cells, plus fainter normal epithelial nuclei which are not of interest. Since it is known that the mitotic nuclei are likely to be much darker than average, only the darkest 10% of blobs are selected for further analysis. This is achieved by sorting the blobs into ascending order of filter output (so the darkest occur first), using a QuickSort algorithm (such as described in Klette R., Zamperoniu P., 'Handbook of Image Processing Operators', John Wiley & Sons, 1996), finding the 10th percentile of the sorted values, and choosing all blobs darker than this percentile.

Segmentation and first clutter rejection

The next processing stage 22 aims to find an approximate segmentation of the image, to separate regions (defined as connected sets of pixels) potentially associated with the cell nuclei of interest, from the background. The full-sized original image (red component) is used at the commencement of this stage.

Firstly, a grey-level threshold is selected. This is achieved by choosing a set of 15x15 pixel neighbourhoods centred on each of the blobs selected at the end of stage 21, collating all pixels within all these neighbourhoods into a single list, and computing the mean grey-level of these pixels.

A new thresholded binary image is now produced. Pixels in the red component of the original image whose grey levels are below (darker than) the threshold mean computed above are set to 1; remaining pixels are set to 0.

Connected component labelling is now applied to this binary image. This is a known image processing technique (such as described in A Rosenfeld and A C Kak, 'Digital Picture Processing', Vols. 1 & 2, Academic Press, New York, 1982) which gives numerical labels to connected regions in the binary image, these being groups of connected pixels whose values are all 1. An 8-connectedness rule is

used, so pixels are deemed to be connected when they are horizontally, vertically, or diagonally adjacent. Each region corresponding to a selected blob from stage 21 is assigned a separate label, enabling pixels belonging to those regions to be identified. The following region properties are then computed:

Area = number of pixels within the region

Thickness = minimum thickness of the region, defined thus: for each pixel in the region, find the minimum distance from that pixel to the outside of the region. Thickness is then defined to be the maximum of these minimum distances. Note that thickness is not the same as width; for a rectangle the thickness is half the width, and for a circle the thickness is the radius.

Regions whose area is less than 190 pixels or whose thickness is less than 4 pixels are rejected, these being too small to be mitotic cell nuclei.

At this stage the mean grey-level of the pixels within each region is also calculated from the red component of the original image. The overall mean and standard deviation of these mean grey-levels is then found for later use in grey-level normalisation (stage 25).

Contour selection

The next processing stage 23 incorporates two levels of contour selection to gain a better representation of the actual shape of the boundary of each remaining object at both low and high resolutions. Firstly, a low-resolution (large-scale) contour is computed, which gives an approximate shape, and secondly a high-resolution (small-scale) contour is found which gives a more accurate boundary representation. Following consistency checks between the two contours, attributes of the boundary are then measured from the small-scale contour.

For each of the objects remaining after stage 22, a local region of interest (ROI) is selected. This ROI is centred on the nominal centre of the object (as found in stage 21), and has an extent of 50 pixels in each direction, the region size being truncated as necessary to ensure the ROI lies within the bounds of the original image. This allows ROIs which would otherwise overlap the edges of the image to be included. Alternatively the ROIs could be defined by taking the regions identified in stage 22 and adding a border of a selected number of pixels. In either

case, it is desirable that the ROIs exceed the size of those regions somewhat in order to ensure the generation of the low-resolution contours.

To find a low-resolution representation for the boundary of each object, the region defined by the ROI above is used to define a sub-image within the output of the blob filter (stage 21). This sub-image will consist of both positive and negative grey levels. Contours at two levels within this sub-image are then sought, namely at levels 0 and –10 which have been found to be best experimentally. By virtue of the operation of the blob filter in stage 21, the zero level contour in the respective sub-image is that contour which exhibits the highest edge strength. A contour is a curve consisting of points of equal value for some given function; in this case the function is defined by the grey-level pixel values. In this embodiment, the Matlab® contour function is employed but any contouring algorithm can be used which returns contours in the same form, as a set of contiguous points ordered around the contour; (Matlab® is a well known computational tool from The MathWorks, Inc.). Matlab® returns a set of locations with sub-pixel resolution which are in order of location around the contour, i.e. traversing the set of locations is equivalent to walking around the contour. Contours are only treated as valid if they satisfy all the following four conditions:

- they form closed loops within the ROI, i.e. the last contour point is the same as the first contour point;
- they are consistent with the location of the object (there is at least one contour point whose distance from the nominal centre of the object is less than or equal to 30 pixels);
- they have a sufficiently similar area to the "nominal area" found from the grey-level segmentation computed in stage 22 (the definition of the area within a contour is given later in this section). The contour area must be at least 50% of the nominal area;
- they have the correct grey-level orientation, namely pixels within the contour are darker than those outside the contour.

The object is retained for further analysis (maintained in list in computer) only if a valid contour is found from at least one of the two contour levels (0 and -10). If both contour levels yield a valid contour, then the latter one (-10) is chosen for further use.

To find a high-resolution representation, the region defined by the ROI above is taken out from the red component of the original image to form a sub-image. Contours are not extracted from the image at its original resolution, because these have been found to be too rough. Instead, the resulting sub-image is expanded in size by a factor of two, using the Matlab® bilinear interpolation function, to give additional resolution. In bilinear interpolation, to find the values of a selected point not on the original image grid, its four nearest grid points are located, and the relative distances from the selected point to each of its four neighbours are computed. These distances are used to provide a weighted average for the grey-level value at the selected point.

This interpolated image is then smoothed before contouring, by correlating (see earlier description with reference to stage 21) with a 3x3 smoothing filter (*s*) defined thus:

$$s = \frac{1}{16}\begin{pmatrix} 1 & 2 & 1 \\ 2 & 4 & 2 \\ 1 & 2 & 1 \end{pmatrix}$$

Valid contours are then sought at each of several threshold levels. The range of threshold levels starts at the minimum grey-level within the sub-image, and increases up to the maximum grey-level in steps of 10 grey levels, so the actual contour levels are set adaptively. Valid contours are defined in the same manner as for the low-resolution boundary above.

Having found a set of valid contours at each threshold level, the edge strength at each point on the contour is estimated. The edge strength at each image pixel is defined as the modulus of the vector gradient of the original red component of the image *I*, where the vector gradient is defined as $\text{grad}I = \left(\frac{\partial I}{\partial x}, \frac{\partial I}{\partial y}\right)$, where the two partial derivatives are obtained from taking differences in pixel grey-level values in the X and Y directions respectively. The edge strength at contour points which lie between image pixels is estimated using bilinear interpolation (as described above) from the nearest pixel values. The mean edge strength around the contour is then computed. The contour having the greatest edge strength is chosen as being the most representative of the boundary of the object. If no valid contours are found, the object is rejected.

A consistency check between the low-resolution and high-resolution contours is then performed. The area within each contour is computed from the boundary contour using Green's Theorem (such as described in Chap 6 in 'Vector Analysis and Cartesian Tensors', D.E.Bourne and P.C.Kendal, 2nd ed, Nelson, 1977). This gives the following formula for area:

$$A = \left| x_n(y_1 - y_n) + \sum_{i=1}^{n-1} x_i(y_{i+1} - y_i) \right|$$

where (x_i, y_i) are the contour points.

These areas are then subjected to the following tests:

High-resolution area > 0.6*low-resolution area

High-resolution area < 1.4* low-resolution area

If either of these tests fail, the object is rejected.

Finally, there is a check that the low- and high-resolution contours for each object overlap sufficiently. For each object, two binary images are formed. The first binary image is formed by setting the value of pixels which lie within the low-resolution contour to 1, and those pixels outside the contour to 0, using the Matlab® function *roipoly*. The second binary image is formed in the same way from the high-resolution contour. The absolute difference of these two images is taken, resulting in another binary image in which pixels are set to 1 if and only if they lie within one of the contours and not the other, and 0 otherwise. Connected component labelling (see stage 22 description) is applied to this new binary image to identify separate regions. The thickness of each of these regions is computed (as in stage 22). If any region thickness exceeds 5 pixels, the corresponding object is rejected.

Simplified visualisations of the effects of the stage 23 processing are shown in Figures 3 and 4.

In Figure 3(a) a local region of interest 30 is defined around the nominal centre 31 of an object 32 which is represented in this Figure by a series of contours. A second object 33 also appears in the same sub-image. Figure 3(b) illustrates the low-resolution boundary contour 34 computed for the object 32 and Figure 3(c) the high-resolution boundary contour 35 computed for the same. Figure 3(d) illustrates the overlap between these two resolutions with the region of difference

36 shaded. In this case the areas within the contours 34 and 35 are sufficiently similar and the thickness of the region 36 is sufficiently small to pass all the above-mentioned consistency checks and the object 32 will be retained. In effect these checks are showing that the object is sufficiently uniformly dark to potentially represent a mitotic cell nucleus. The object 33 will not be treated as valid for the ROI 30 because its contours are not consistent with the centre 31. It will, however, be separately analysed within a separate ROI (not shown) defined around its own nominal centre.

In Figure 4(a) there is another example of a local region of interest 40 defined around an object 41. Figure 4(b) illustrates the low-resolution boundary contour 42 computed for this object and Figure 4(c) the high-resolution boundary contour 43. In this case the area of the contour 43 is substantially less than that of the contour 42 (approximately 0.4) so it fails the first of the above-mentioned consistency checks and the object 41 will not be processed further. This is indicative of a normal epithelial cell nucleus which has a relatively darker nucleolus (chosen as the high-resolution boundary because of its high edge strength) surrounded by a less dark region (chosen as the low-resolution boundary).

Boundary tracking

The next processing stage 24 applies a tracking algorithm to the high-resolution contour representing the object's boundary for each object retained from the previous stage 23 in order to estimate curvature. The aim is to smooth the boundary and then measure curvature, because simply calculating curvature from the contour segments gives too rough a measurement. For the identification of mitotic cell nuclei the degree of non-convexity of the boundary is of interest, so the latter method of calculation is inappropriate.

The particular algorithm which has been used in the preferred embodiment is based on a Probability Density Association Filter (PDAF), such as described in Y.Bar-Shalom and T.E.Fortmann, "Tracking and Data Association", Mathematics in Science and Engineering series, vol 179, Orlando, Fl., Academic Press, 1988. This type of tracking algorithm is designed to estimate the parameters of a chosen object (target) in the presence of other measurements which are not related to the object in question (noise and clutter). In this case the 'target' state variables are the position, orientation and curvature of the object's boundary, and the measurements

are the positions of the contour points and the orientations of the lines joining each pair of contour points.

The PDAF filter requires a model for the dynamics of the boundary state. The boundary dynamics is given by a constant curvature (the radius of curvature is set to 10 pixels) plus an assumed random perturbation known as system noise. This noise is determined by the variance of curvature perturbation, which is chosen according to how irregular the boundary of a mitotic cell nucleus is expected to be. In the preferred embodiment the curvature variance is 9 for position and 0.09 for angle (in radians).

As a starting point, it is assumed that for each object potentially representing a mitotic cell nucleus a connected set of edge features has been extracted from the image. In this case, edge features are line segments joining two adjacent contour points. Each edge feature has the following measurements that were made as part of the contour extraction process:

- Position x_m, y_m (horizontal and vertical image coordinates) of the centre of the edge
- Orientation θ_m, i.e. the angle between the edge and the horizontal.

The purpose of the tracker is to estimate the most likely true location, orientation and curvature x_s, y_s, θ_s,κ of the boundary at each point from the above measurements, given that there are measurement errors with an assumed Gaussian distribution. The following information vectors are defined:

- The measurement vector $z = (x_m, y_m, \theta_m)$;
- The system state vector $x = (x_s, y_s, \theta_s, \kappa)$.

To use the PDAF filter to do this, the following information about the true boundary and the measurement process is required:

- The relationship between the position, orientation and curvature of neighbouring points on the boundary (the system model). This incorporates a transition matrix Φ linking neighbouring states x and a system noise model that adds extra random perturbations to x.

- The relationship between the measurement vector z and the system state x. This incorporates a transition matrix H linking x to z and a measurement noise model that adds extra random perturbations to z.

- It is assumed that not all of the edge features are associated with the nuclear boundary; the ones that are not are denoted clutter.

In its most general form the PDAF processes several measurements z at each step in estimating x. In this case only one edge feature is processed at a time, so there are only two hypotheses to be tested; either the feature is from clutter or from the real nuclear boundary.

The system transition matrix Φ is based on constant curvature, so to predict a neighbouring system state the unique circle or straight line with curvature κ, tangent slope θ_s going through the point x_s, y_s is extrapolated to the point that is closest to the next measurement point.

The system noise has a Gaussian distribution with zero mean and a covariance matrix based on independent perturbations in curvature, orientation and lateral offset (movement in a direction normal to the boundary). A Brownian model is used, where the standard deviations of perturbations in curvature, orientation and lateral offset are proportional to the square root of the arc length of the extrapolated circle of the previous paragraph. The accumulated effect of curvature perturbation on orientation and lateral offset is also modelled, resulting in the following covariance matrix:

$$Q = \sigma_k^{\,2}\begin{pmatrix} s & \frac{1}{2}s^2 & \frac{1}{6}s^3 \\ \frac{1}{2}s^2 & \frac{1}{3}s^3 & \frac{1}{8}s^4 \\ \frac{1}{6}s^3 & \frac{1}{8}s^4 & \frac{1}{20}s^5 \end{pmatrix} + s\begin{pmatrix} 0 & 0 & 0 \\ 0 & \sigma_{s\theta}^{\,2} & 0 \\ 0 & 0 & \sigma_{sy}^{\,2} \end{pmatrix}$$

with respect to the system curvature κ, system slope θ and lateral offset respectively, where s is the arc length (the circular distance between the previous point and the estimate of the next point). The constants σ_k, $\sigma_{s\theta}$, σ_{sy} define the average roughness of the nuclear boundary, and depend on the type of cell being analysed.

The measurement transition matrix H maps the system parameters to the measurement parameters in the natural way:

$$\begin{pmatrix} x_m \\ y_m \\ \theta_m \end{pmatrix} = H \begin{pmatrix} x_s \\ y_s \\ \theta_s \\ \kappa \end{pmatrix}, \quad H = \begin{pmatrix} 1 & 0 & 0 & 0 \\ 0 & 1 & 0 & 0 \\ 0 & 0 & 1 & 0 \end{pmatrix}$$

The measurement noise is based on independently Gaussian distributed perturbations of slope and lateral offset, resulting in the following covariance matrix with respect to measurement slope and lateral offset respectively:

$$R = \begin{pmatrix} \sigma_{m\theta}{}^2 & 0 \\ 0 & \sigma_{my}{}^2 \end{pmatrix}$$

The constants $\sigma_{m\theta}$, σ_{my} define the average smoothness of the nuclear boundary, and depend on the type of cell being analysed.

The following constants are used to define the clutter model:

- ρ = Clutter density = average number of edges per unit area that are not associated with the nuclear boundary.
- P_D = Probability that the edge feature is associated with the true nuclear boundary.

These constants depend on the clutter present in the image, both its edge strength relative to the nuclear boundary and its average spatial density.

For a nucleus with average radius r the following parameters of the above model are used (all units are image pixels):

- $\sigma_k = r^{3/2}$
- $\sigma_{my} = 3$
- $\sigma_{m\theta} = 0.3$ radians
- $\sigma_{sy} = 0.9$
- $\sigma_{s\theta} = 0.09$ radians
- $\rho = 0.01$

- $P_D = 0.8$

The initial value for the system covariance matrix M is given by:

$$M_0 = \begin{pmatrix} \sigma_{my}^2 & 0 & 0 \\ 0 & \sigma_{m\theta}^2 & 0 \\ 0 & 0 & \sigma_{k0}^2 \end{pmatrix}, \text{where } \sigma_{k0} = 1/r$$

The PDAF estimator is now applied sequentially as follows. The matrices H_k, Q_k and R_k are all constant in this application (as defined above). The following expressions are those known from the Bar-Shalom and Fortmann reference quoted above.

Update:

INNOVATION

$$\underline{\nu}'_k = \sum_{i=1}^{N_k} \beta_{ki}\, \underline{\nu}_{ki} \quad \text{where} \quad \underline{\nu}_{ki} = \underline{z}_{ki} - H_k \underline{\bar{x}}_k$$

KALMAN GAIN MATRIX

$$K_k = M_k\, H_k^T\, S_k^{-1} \quad \text{where} \quad S_k = H_k\, M_k\, H_k^T + R_k$$

BETA WEIGHTS

$$\beta_{ki} = \begin{cases} e_{ki} / [\, b + \sum_{j=1}^{N_k} e_{kj} \,] & \text{for } i \neq 0 \\ b \;\; / [\, b + \sum_{j=1}^{N_k} e_{kj} \,] & \text{for } i = 0 \end{cases}$$

where $e_{ki} = \exp\left(-\tfrac{1}{2} \underline{\nu}_{ki}^T S_k^{-1} \underline{\nu}_{ki}\right)$ for $i \neq 0$, and $b = \rho(1 - P_D)\sqrt{|2\pi S_k|} / P_D 2$

STATE ESTIMATE UPDATE

$$\underline{\hat{x}}_k = \underline{\bar{x}}_k + K_k\, \underline{\nu}'_k$$

ERROR COVARIANCE UPDATE

$$P_k = \beta_{k0} M_k + (1-\beta_{k0}) P^* + K_k \left[\left(\sum_{i=1}^{N_k} \beta_{ki} \underline{\nu}_{ki} \underline{\nu}_{ki}^T \right) - \underline{\nu'}_k \underline{\nu'}_k^T \right] K_k^T$$

where $P^* = [I - K_k H_k] M_k$

Prediction:

STATE ESTIMATE EXTRAPOLATION

$$\underline{\bar{x}}_{k+1} = \Phi_k \underline{\hat{x}}_k$$

ERROR COVARIANCE EXTRAPOLATION

$$M_{k+1} = \Phi_k P_k \Phi_k^T + Q_k$$

This process continues until the entire contour is traversed (i.e. returned to the starting point). This is then repeated around the contour for a second time (using the final conditions from the first pass as starting conditions for the second pass); this ensures that the final estimate of the smoothed contour is independent of the assumed initial conditions.

The curvature of the smoothed contour derived from the PDAF tracker is now used to find a measure of the degree of non-convexity of the object's boundary. Firstly, the sign of the curvature is set so that it is positive where the boundary is locally convex and negative where locally concave (as viewed from outside the boundary). All positive values of curvature are then set to zero, leaving non-zero values only at locations where the boundary is locally concave. A graph of curvature (Y-axis) against perimeter arc length i.e. distance along the boundary (X-axis) is plotted, then the line integral of curvature with respect to arc length is computed. The absolute value of this integral is taken to produce a non-negative result. The final result is a dimensionless quantity giving an indication of overall non-convexity, called the "negative curvature area". Objects which are almost completely convex, in this case whose negative curvature area is less than 0.2, are then rejected.

The output from this process is a set of boundary measurements for each object, namely negative curvature area, and a more precise estimate of area.

Grey-level normalisation

Next a normalisation process 25 is carried out to allow for differences in overall brightness between different slides. For each remaining object, the mean grey level of the pixels enclosed within (but not on) the high-resolution contour found in stage 23 is calculated. The statistics used for normalisation are the overall mean and standard deviation of the grey levels of the regions obtained from stage 22. Each object's grey level is then normalised (by subtracting this mean and dividing by this standard deviation). The output is a statistic for each assumed nucleus.

Second clutter rejection

The next process 26 involves a second stage of classification and clutter rejection based on the Fisher classifier to discriminate between objects representing mitotic and non-mitotic nuclei. The Fisher classifier is a known statistical classification method described for example in Section 4.3 of "Statistical Pattern Recognition" by Andrew R. Webb, Arnold Press, 1999, and is preferred for this stage of the process due to its robustness against overtraining.

In this case the Fisher classifier uses a set of information about each object that has been derived by analysis as described above. Each information set is a feature vector, that is an ordered list of real numbers each describing some aspect of the object; each component number is denoted an object feature. The purpose of the classification algorithm is to discriminate between two classes of object based on the information contained in their feature vectors. The output of the algorithm is a set of numbers, one for each object, indicating the likelihood that the nucleus which it represents is a member of one of the two chosen classes (in this case the classes are mitotic and non-mitotic).

For a given feature vector x, the standard implementation of the Fisher classifier output is defined as:

$$F = \sum_{k=1}^{n} a_k x_k$$

where $x=[x_1, \ldots x_k]$ is the feature vector. In this embodiment, this definition has been extended to use non-linear functions of the feature vector, namely:

$$F = \sum_{k=1}^{n} a_k g_k(x)$$

where a_k are prescribed real numbers and g_k are prescribed functions of the feature vector x. These functions and variables are chosen to give the lowest number of misclassifications for objects with known class.

The components of the feature vector x are mean grey level (computed in stage 25) and negative curvature area (computed in stage 24). In principle area could also be used, since smaller mitotic cell nuclei tend to be darker and less concave than larger ones. In this case a quadratic set of basis functions (g_k) are used, so that the Fisher classifier value is given by:

$$F = a_1 G + a_2 G^2 + a_3 C + a_4 GC + a_5 C^2 + a_6$$

where G is the normalised grey-level, C is the negative curvature area, and the coefficients a_i are derived from the training stage referred to below.

The coefficients and decision boundary for the Fisher classifier are obtained by training the classifier on a large number of example slides provided by a histopathologist where accurate ground truth (sets of mitotic and non-mitotic cells) is also available. The training stage results in a classifier boundary which minimises the total number of misclassifications, i.e. both false negatives (missed mitotic cells) and false positives (falsely-detected non-mitotic cells). In the preferred embodiment the resulting coefficients a_i that have been derived from this training stage are [-0.87431, 0.10205, 0.84614, -0.18744, -0.04954, -5.56334]. Figure 5 illustrates the classifier together with the data on which it was trained, where plusses indicate mitotic cells and crosses indicate non-mitotic cells.

Mitosis count

Stage 27 counts the number of objects deemed to represent the nuclei of mitotic cells, that is to say only those objects whose values exceed a given threshold in the output of the Fisher classifier. The preferred criterion is $F>0$ (illustrated as the decision boundary in Figure 5), set to give the optimum trade-off between missed mitotic cells and falsely-detected non-mitotic cells. The number of objects whose

classifier value exceeds this threshold defines the mitotic count for that tile. The count for the ten tiles analysed is aggregated, and can be converted into an indication of cancer grade in accordance with a table as previously described in connection with the existing manual procedure.

5

It will be appreciated that the coding of a computer program to implement all of the processing stages described above for the preferred embodiment of the invention can be achieved by a skilled programmer in accordance with conventional techniques. Such a program and code will therefore not be described further.

CLAIMS

1. A method for the automated analysis of a digital image comprising an array of pixels, including the steps of:

(a) identifying the locations of objects within the image which have specified intensity and size characteristics;

(b) defining regions of specified extent within the image which contain respective said objects;

(c) deriving from the data within respective said regions one or more respective closed contours comprising points of equal intensities; and

(d) estimating the curvature of at least one respective said contour within respective said regions at least to produce a measure of any concavity thereof.

2. A method according to claim 1 wherein step (a) comprises the application of a radially-symmetric difference filter with zero mean.

3. A method according to claim 2 wherein the image is filtered at a plurality of resolutions of increasing scale.

4. A method according to claim 2 or claim 3 wherein said locations are identified in accordance with the locations of respective local extrema in the output of said filter.

5. A method according to claim 4 including the step of sorting, in order of intensity, local extrema in the output of said filter and selecting for further analysis only those objects which correspond to a specified proportion of said extrema in such order.

6. A method according to any preceding claim further comprising, following step (a):

selecting an intensity threshold related to the mean intensity of pixels within the image in neighbourhoods of said locations;

creating a binary image according to whether pixels in the first-mentioned image are above or below said threshold;

identifying regions in the binary image composed of connected pixels which are below said threshold in the first-mentioned image; and

rejecting from further analysis those objects which correspond to such regions in the binary image which fall below a specified size or thickness.

7. A method according to any preceding claim wherein step (c) comprises, for respective said regions, deriving respective first and second said contours having respectively lower and higher resolutions, determining whether the sizes and locations of said first and second contours are consistent within specified criteria and, if so consistent, selecting said second contour for step (d).

8. A method according to claim 7 wherein, for respective said regions, the first said contour is derived by:

seeking within the region one or more contours of respective specified intensities;

determining whether the or each such contour is a closed contour and meets specified location, size and/or intensity orientation criteria; and

if more than one such contour is a closed contour and meets such criteria, selecting from the same the contour of the lowest intensity.

9. A method according to claim 8 wherein said specified intensities are no greater than that which corresponds to the contour of highest edge strength within the respective region.

10. A method according to claim 9 when appended to any one of claims 2 to 5 wherein said first contour is derived by seeking one or more contours in the output of said filter for the respective region and said specified intensities are no greater than the zero level in such output.

11. A method according to any one of claims 8 to 10 wherein, for respective said regions, the second said contour is derived by:

seeking within the region a plurality of contours of respective specified intensities ranging between the lowest and highest intensities within the region;

determining whether each such contour is a closed contour and meets specified location, size and/or intensity orientation criteria; and

if more than one such contour is a closed contour and meets such criteria, selecting from the same the contour having the highest edge strength.

12. A method according to any preceding claim wherein step (d) includes the application of a Probability Density Association Filter to respective said contours.

13. A method according to any preceding claim wherein step (d) comprises, for respective said contours:

measuring the curvature of the contour at a plurality of points around the contour, convexity and concavity being of opposite sign;

setting convex values of such curvature to zero;

plotting resultant values of curvature at said points against a measure of the distance of the respective point along the contour; and

computing as said measure of concavity the line integral of such plot.

14. A method according to any preceding claim further comprising the step of:

(e) classifying objects into one of at least two classes in accordance with a function of said measure of concavity of a contour corresponding to the respective object and a measure of the mean intensity of the respective object.

15. A method according to claim 14 wherein step (e) is performed by use of a Fisher classifier.

16. A method according to claim 14 or claim 15 wherein the intensities of respective objects are normalised prior to step (e).

17. A method according to any one of claims 14 to 16 further comprising the step of:

(f) counting the number of objects classified into a specified one of said classes.

18. A method according to any preceding claim for the automated analysis of a digital image of a histological or cytology specimen.

19. A method according to claim 18 wherein the image is of a section of breast tissue.

20. A method according to claim 18 or claim 19 when appended to claim 17, wherein said specified class is identified as the class of mitotic epithelial cell nuclei.

21. A method according to any one of claims 1 to 17 for the automated analysis of a digital image of a soil sample.

22. A method for the automated identification of mitotic activity from a digital image of a histological specimen, including the steps of:

(a) identifying the locations of objects within the image which have specified intensity and size characteristics associated with epithelial cell nuclei;

(b) defining regions of specified extent within the image which contain respective said objects;

(c) deriving from the data within respective said regions one or more respective closed contours comprising points of equal intensities;

(d) estimating the curvature of at least one respective said contour within respective said regions at least to produce a measure of any concavity thereof; and

(e) classifying objects as representing mitotic cell nuclei as a function of at least said measure of concavity of a contour corresponding to the respective object.

23. Apparatus for the automated analysis of a digital image comprising means adapted to perform a method according to any preceding claim.

24. A computer program product comprising a computer readable medium having thereon computer program code means adapted to cause a computer to execute a method according to any one of claims 1 to 22.

25. A computer program comprising instructions to cause a computer to execute a method according to any one of claims 1 to 22.

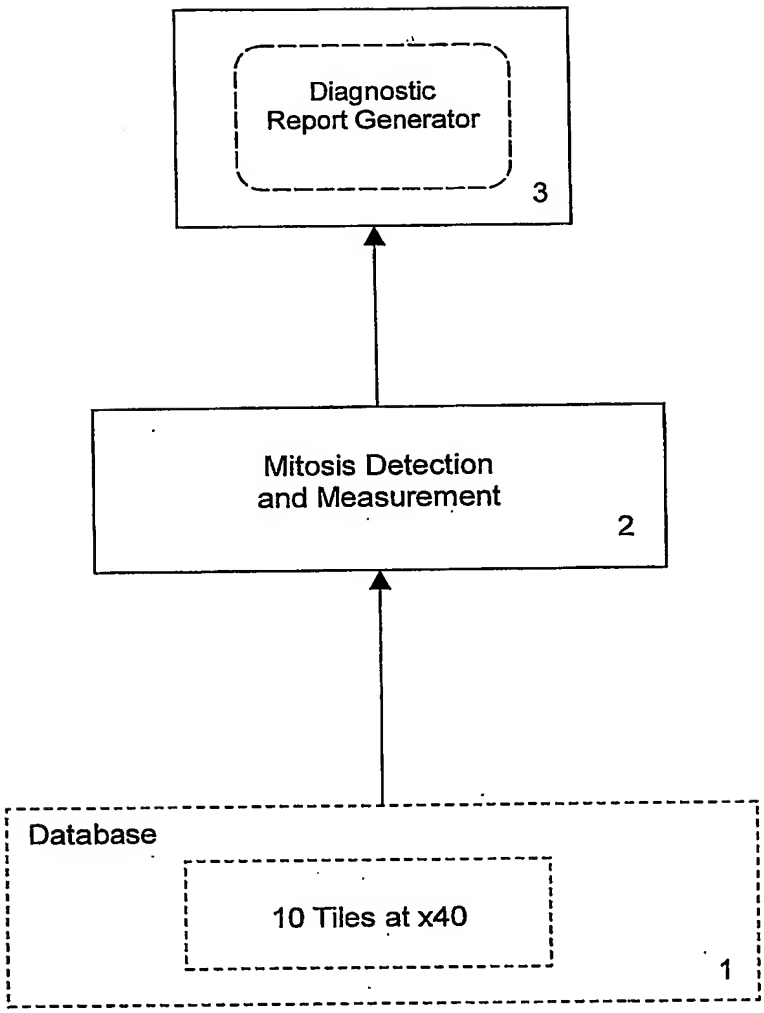
Diagnostic
Report Generator
3
Mitosis Detection
and Measurement
2
Database
10 Tiles at x40
1

Figure 1

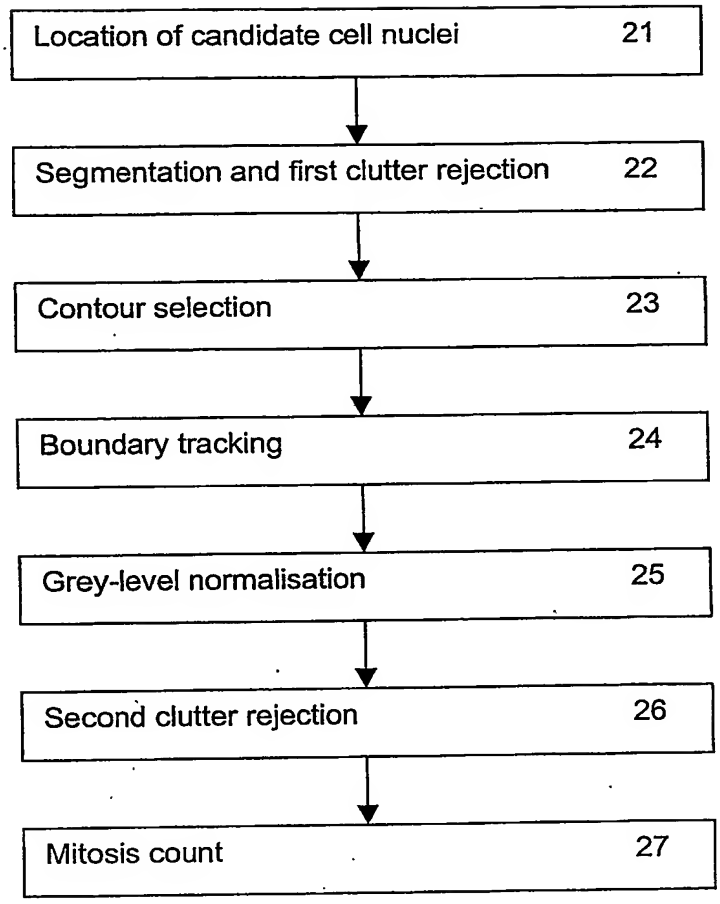
Location of candidate cell nuclei 21
Segmentation and first clutter rejection 22
Contour selection 23
Boundary tracking 24
Grey-level normalisation 25
Second clutter rejection 26
Mitosis count 27

Figure 2

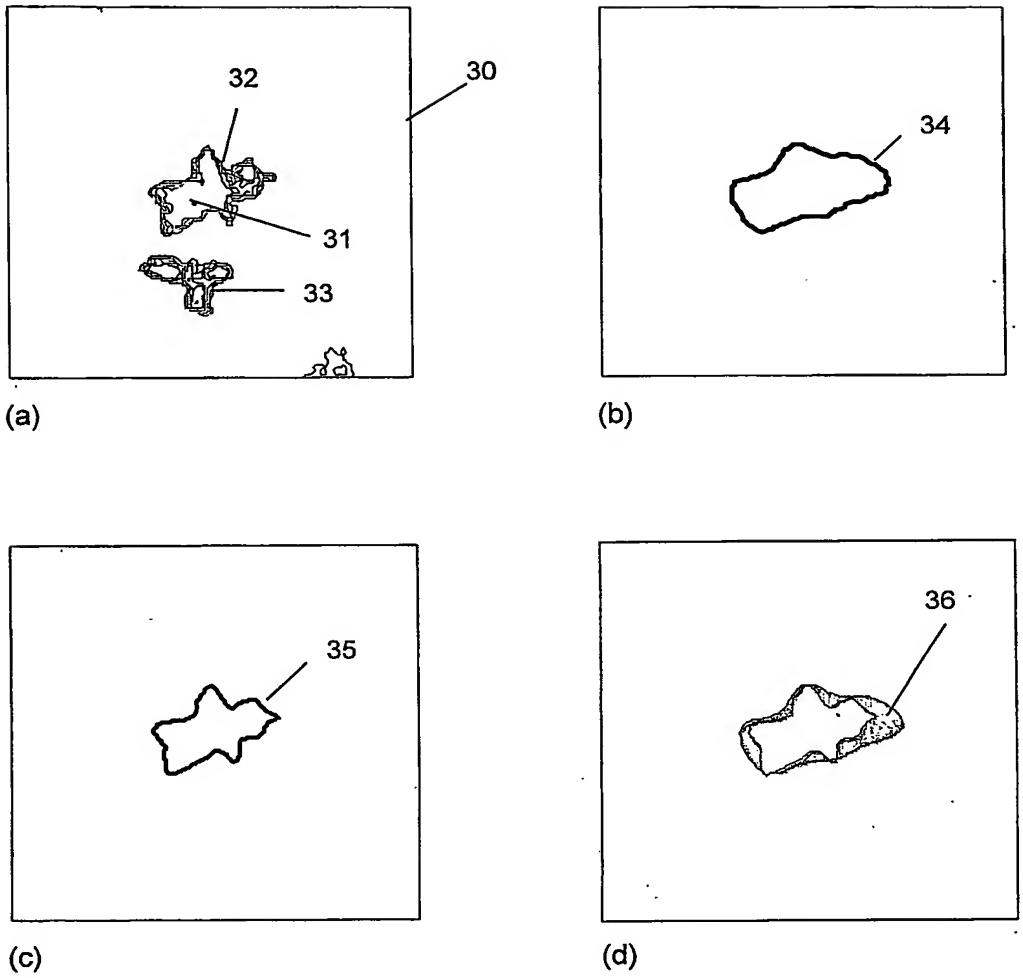

Figure 3

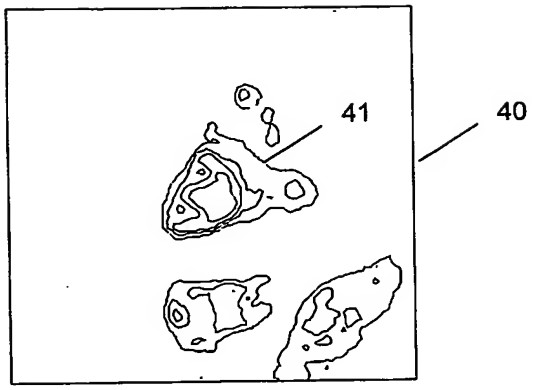

(a)

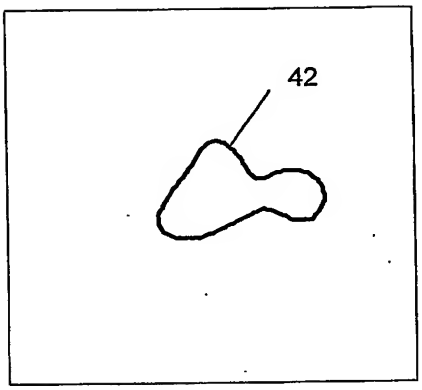

(b)

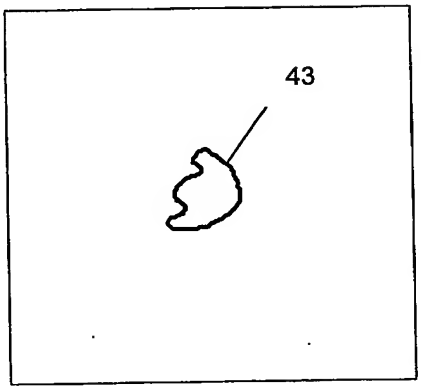

(c)

Figure 4

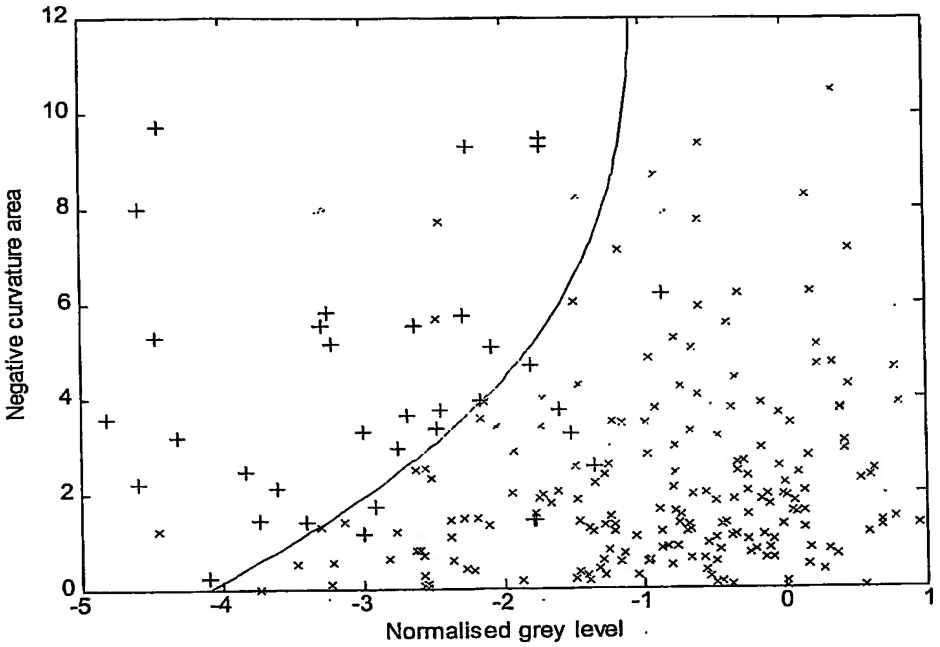
Negative curvature area
Normalised grey level
12
10
8
6
4
2
0
-5
-4
-3
-2
-1
0
1

Figure 5

(12) INTERNATIONAL APPLICATION PUBLISHED UNDER THE PATENT COOPERATION TREATY (PCT)

(19) World Intellectual Property Organization
International Bureau

(43) International Publication Date
1 July 2004 (01.07.2004)

PCT

(10) International Publication Number
WO 2004/055733 A3

(51) International Patent Classification[7]: G06T 7/00

(21) International Application Number:
PCT/GB2003/005445

(22) International Filing Date:
12 December 2003 (12.12.2003)

(25) Filing Language: English

(26) Publication Language: English

(30) Priority Data:
0229338.9 17 December 2002 (17.12.2002) GB

(71) Applicant *(for all designated States except US)*: **QINETIQ LIMITED** [GB/GB]; 85 Buckingham Gate, London SW1E 6PD (GB).

(72) Inventors; and

(75) Inventors/Applicants *(for US only)*: **WATSON, Sharon, Katrina** [GB/GB]; QinetiQ Limited, Cody Technology Park, Rm 1010 Building A9, Ively Road, Farnborough, Hampshire GU14 0LX (GB). **WATSON, Graham, Howard** [GB/GB]; QinetiQ Limited, Cody Technology Park, Rm 1008 Building A9, Ively Road, Farnborough, Hampshire GU14 0LX (GB).

(74) Agent: **OBEE, Robert, W.**; IP QinetiQ Formalities, Cody Technology Park, A4 Building, Room G016, Ively Road, Farnborough, Hampshire GU14 0LX (GB).

(81) Designated States *(national)*: AE, AG, AL, AM, AT, AU, AZ, BA, BB, BG, BR, BW, BY, BZ, CA, CH, CN, CO, CR, CU, CZ, DE, DK, DM, DZ, EC, EE, EG, ES, FI, GB, GD, GE, GH, GM, HR, HU, ID, IL, IN, IS, JP, KE, KG, KP, KR, KZ, LC, LK, LR, LS, LT, LU, LV, MA, MD, MG, MK, MN, MW, MX, MZ, NI, NO, NZ, OM, PG, PH, PL, PT, RO, RU, SC, SD, SE, SG, SK, SL, SY, TJ, TM, TN, TR, TT, TZ, UA, UG, US, UZ, VC, VN, YU, ZA, ZM, ZW.

(84) Designated States *(regional)*: ARIPO patent (BW, GH, GM, KE, LS, MW, MZ, SD, SL, SZ, TZ, UG, ZM, ZW),

[Continued on next page]

(54) Title: ASSESSING OF MITOTIC ACTIVITY BY IMAGE ANALYSIS

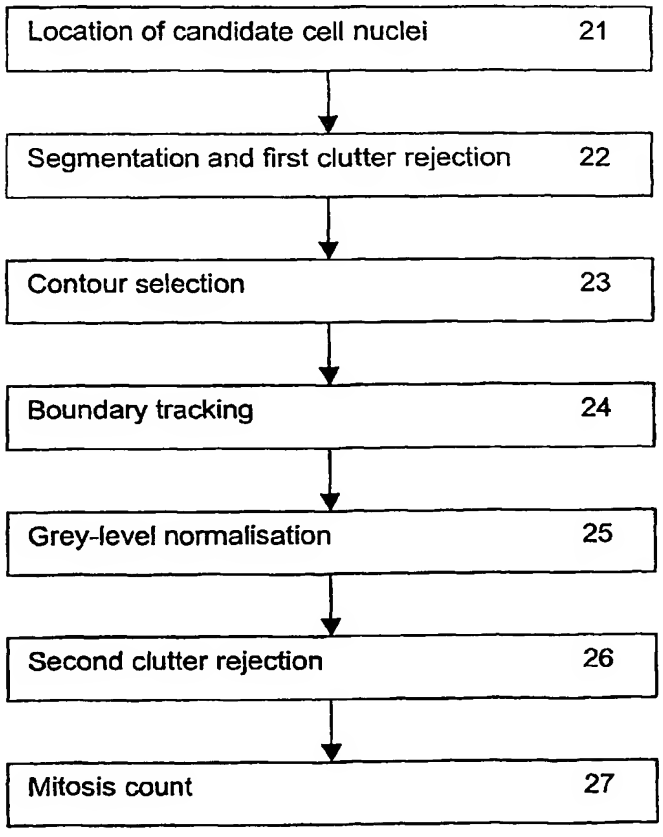

(57) Abstract: A method for the automated analysis of digital images, particularly for the purpose of assessing mitotic activity from images of histological slides for prognostication of breast cancer. The method includes the steps of identifying the locations of objects within the image which have intensity and size characteristics consistent with mitotic epithelial cell nuclei, taking the darkest 10 % of those objects, deriving contours indicating their boundary shape, and smoothing and measuring the curvature around the boundaries using a Probability Density Association Filter (PDAF). The PDAF output is used to compute a measure of any concavity of the boundary - a good indicator of mitosis. Objects are finally classified as representing mitotic nuclei or not, as a function of boundary concavity and mean intensity, by use of a Fisher classifier trained on known examples. Other uses for the method could include the analysis of images of soil samples containing certain types of seeds or other particles.

WO 2004/055733 A3

Eurasian patent (AM, AZ, BY, KG, KZ, MD, RU, TJ, TM), European patent (AT, BE, BG, CH, CY, CZ, DE, DK, EE, ES, FI, FR, GB, GR, HU, IE, IT, LU, MC, NL, PT, RO, SE, SI, SK, TR), OAPI patent (BF, BJ, CF, CG, CI, CM, GA, GN, GQ, GW, ML, MR, NE, SN, TD, TG).

Declaration under Rule 4.17:

— *of inventorship (Rule 4.17(iv)) for US only*

Published:

— *with international search report*

— *before the expiration of the time limit for amending the claims and to be republished in the event of receipt of amendments*

(88) Date of publication of the international search report:
19 May 2005

For two-letter codes and other abbreviations, refer to the "Guidance Notes on Codes and Abbreviations" appearing at the beginning of each regular issue of the PCT Gazette.

INTERNATIONAL SEARCH REPORT

International Application No
GB 03/05445

A. CLASSIFICATION OF SUBJECT MATTER
IPC 7 G06T7/00

According to International Patent Classification (IPC) or to both national classification and IPC

B. FIELDS SEARCHED

Minimum documentation searched (classification system followed by classification symbols)
IPC 7 G06T

Documentation searched other than minimum documentation to the extent that such documents are included in the fields searched

Electronic data base consulted during the international search (name of data base and, where practical, search terms used)
EPO-Internal, INSPEC, WPI Data

C. DOCUMENTS CONSIDERED TO BE RELEVANT

Category °	Citation of document, with indication, where appropriate, of the relevant passages	Relevant to claim No.
X	MADACHY R J ET AL: "Image analysis for automatic classification of mitotic cervical cells" PROCEEDINGS OF THE ANNUAL INTERNATIONAL CONFERENCE OF THE IEEE ENGINEERING IN MEDICINE AND BIOLOGY SOCIETY (IEEE CAT. NO.88CH2566-8) IEEE NEW YORK, NY, USA, 1988, pages 372-374 vol.1, XP010074652 section: "Method" section: "Cell Feature Analysis" section: Cell Classification" ----- -/--	1,6,18, 19,21

[X] Further documents are listed in the continuation of box C.

[ ] Patent family members are listed in annex.

° Special categories of cited documents :

"A" document defining the general state of the art which is not considered to be of particular relevance

"E" earlier document but published on or after the international filing date

"L" document which may throw doubts on priority claim(s) or which is cited to establish the publication date of another citation or other special reason (as specified)

"O" document referring to an oral disclosure, use, exhibition or other means

"P" document published prior to the international filing date but later than the priority date claimed

"T" later document published after the international filing date or priority date and not in conflict with the application but cited to understand the principle or theory underlying the invention

"X" document of particular relevance; the claimed invention cannot be considered novel or cannot be considered to involve an inventive step when the document is taken alone

"Y" document of particular relevance; the claimed invention cannot be considered to involve an inventive step when the document is combined with one or more other such documents, such combination being obvious to a person skilled in the art.

"&" document member of the same patent family

Date of the actual completion of the international search	Date of mailing of the international search report
12 November 2004	29.03.05

Name and mailing address of the ISA	Authorized officer
European Patent Office, P.B. 5818 Patentlaan 2 NL - 2280 HV Rijswijk Tel. (+31-70) 340-2040, Tx. 31 651 epo nl, Fax: (+31-70) 340-3016	Gao, M

Form PCT/ISA/210 (second sheet) (January 2004)

C.(Continuation) DOCUMENTS CONSIDERED TO BE RELEVANT

Category °	Citation of document, with indication, where appropriate, of the relevant passages	Relevant to claim No.
X	HIBBARD L S ET AL: "MULTISCALE DETECTION AND ANALYSIS OF THE SENILE PLAQUES OF ALZHEIMER'S DISEASE" IEEE TRANSACTIONS ON BIOMEDICAL ENGINEERING, IEEE INC. NEW YORK, US, vol. 42, no. 12, 1 December 1995 (1995-12-01), pages 1218-1225, XP000556862 ISSN: 0018-9294 section II. A. "SP detection/classification strategy" section II. C. "SP detection by multiscale template correlation" section II. D. "Detected object definition" section II. G. "Classifier features"	1
Y		2-5

Y	DATABASE MEDLINE [Online] US NATIONAL LIBRARY OF MEDICINE (NLM), BETHESDA, MD, US; September 1999 (1999-09), NETSCH T ET AL: "Scale-space signatures for the detection of clustered microcalculations in digital mammograms." XP002301991 Database accession no. NLM10571382 abstract -& IEEE TRANSACTIONS ON MEDICAL IMAGING. SEP 1999, vol. 18, no. 9, September 1999 (1999-09), pages 774-786, XP002302593 ISSN: 0278-0062 section: III.A "Motivation and outline" section: III.B "Laplacian scale-space" section: III.C "Spot detection"	2-5

A	LINDEBERG T: "FEATURE DETECTION WITH AUTOMATIC SCALE SELECTION" INTERNATIONAL JOURNAL OF COMPUTER VISION, KLUWER ACADEMIC PUBLISHERS, NORWELL, US, vol. 30, no. 2, November 1998 (1998-11), pages 79-116, XP000800306 ISSN: 0920-5691 sections 4-5	1-6,18, 19,21

A	J.G. JONES ET AL: "multiresolution analysis of remotely sensed imagery" INTERNATIONAL JOURNAL OF REMOTE SENSING, 1991, pages 107-124, XP008037183 cited in the application section 2	1-6,18, 19,21

INTERNATIONAL SEARCH REPORT

tional application No.
PCT/GB 03/05445

Box I Observations where certain claims were found unsearchable (Continuation of item 1 of first sheet)

This International Search Report has not been established in respect of certain claims under Article 17(2)(a) for the following reasons:

1. ☐ Claims Nos.:
because they relate to subject matter not required to be searched by this Authority, namely:

2. ☐ Claims Nos.:
because they relate to parts of the International Application that do not comply with the prescribed requirements to such an extent that no meaningful International Search can be carried out, specifically:

3. ☐ Claims Nos.:
because they are dependent claims and are not drafted in accordance with the second and third sentences of Rule 6.4(a).

Box II Observations where unity of invention is lacking (Continuation of item 2 of first sheet)

This International Searching Authority found multiple inventions in this international application, as follows:

see additional sheet

1. ☐ As all required additional search fees were timely paid by the applicant, this International Search Report covers all searchable claims.

2. ☐ As all searchable claims could be searched without effort justifying an additional fee, this Authority did not invite payment of any additional fee.

3. ☐ As only some of the required additional search fees were timely paid by the applicant, this International Search Report covers only those claims for which fees were paid, specifically claims Nos.:

4. ☒ No required additional search fees were timely paid by the applicant. Consequently, this International Search Report is restricted to the invention first mentioned in the claims; it is covered by claims Nos.:

1, 2-6 (when dependent on claim 1), 19, 21 (when dependent on claim 1)

Remark on Protest

☐ The additional search fees were accompanied by the applicant's protest.

☐ No protest accompanied the payment of additional search fees.

FURTHER INFORMATION CONTINUED FROM PCT/ISA/ 210

This International Searching Authority found multiple (groups of) inventions in this international application, as follows:

1. claims: 1, 2-6,18(when dependent on clm 1),19,21(when dependent on clm 1)

   Detection of potential regions of interest
   ---

2. claims: 7(when dependent on clm 1)-11

   contour estimation of the detected objects
   ---

3. claims: 12(when dependent on clm 1),13(when dependent on clm 1),14(when dependent on clm 1)-17,18(when dependent on clm 17),19(when dependent on clm 17),20

   curvature estimation of the contours
